SUPPORTING INFORMATION

Bilayer mass transport model for determining swelling and diffusion in coated, ultrathin membranes

Nichole K. Nadermann, Edwin P. Chan*, Christopher M. Stafford*

Materials Science and Engineering Division, National Institute of Standards and Technology,

100 Bureau Drive, MS 8542, Gaithersburg, MD 20899

(*) Corresponding authors:
Edwin P. Chan
Materials Science and Engineering Division
National Institute of Standards and Technology
100 Bureau Drive, MS 8542
Gaithersburg, MD 20899
E-mail: edwin.chan@nist.gov

Christopher M. Stafford
Materials Science and Engineering Division
National Institute of Standards and Technology
100 Bureau Drive, MS 8542
Gaithersburg, MD 20899
E-mail: christopher.stafford@nist.gov

I. The hydroxyl-rich coating

Commercial RO membranes are often coated with a hydrophilic layer, most likely to reduce fouling by reducing the roughness as well as to serve as a getter-layer. The presence of a coating was indicated via spectroscopy and directly imaged using TEM. PM-IRRAS analysis shows the presence of an OH peak when the sample is equilibrated in dry nitrogen. As there are no -OH groups in PA, this indicates the presence of another material that is rich in OH. Cross-sectional TEM images of the TFC membrane show an additional layer of material between the PA membrane and epoxy resin in which the sample was embedded.

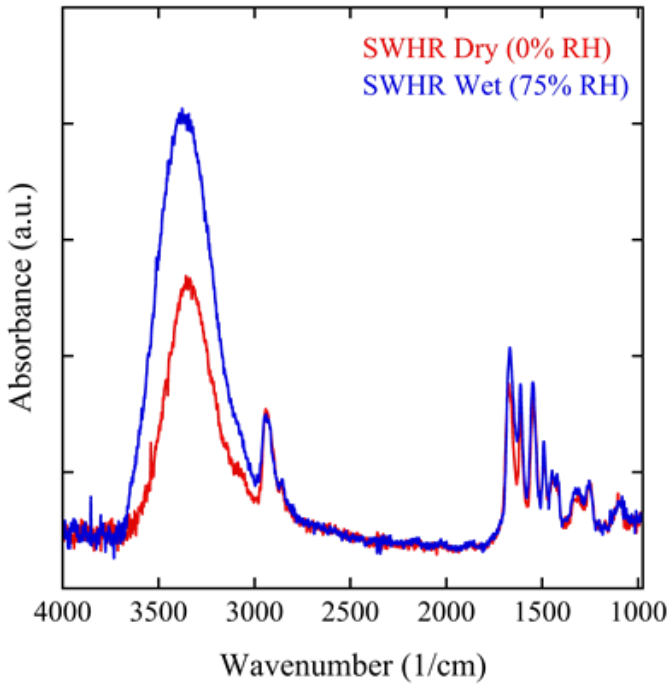

Figure 1. PM-IRRAS analysis of SWHR membrane in 0 %RH and 75 %RH water vapor environments. The presence of the large OH peak in 0 %RH indicates the presence of an additional OH rich layer on the SWHR membrane.

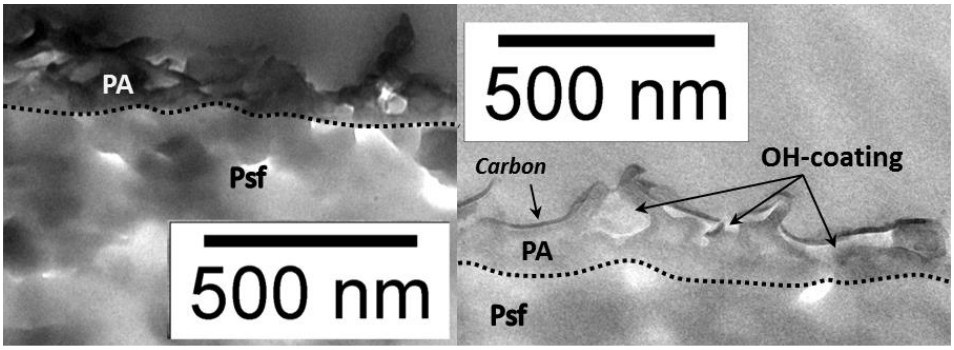

Figure 2. Cross-sectional TEM images of the TFC studied in this work. *Left*: TFC membrane in an epoxy resin matrix. The PA selective layer sits atop the polysulfone support. *Right*: Due to the similarly low electron densities of the OH-coating and the epoxy matrix, a thin layer of carbon was sputter-deposited to provide contrast between the OH-coating and epoxy matrix.

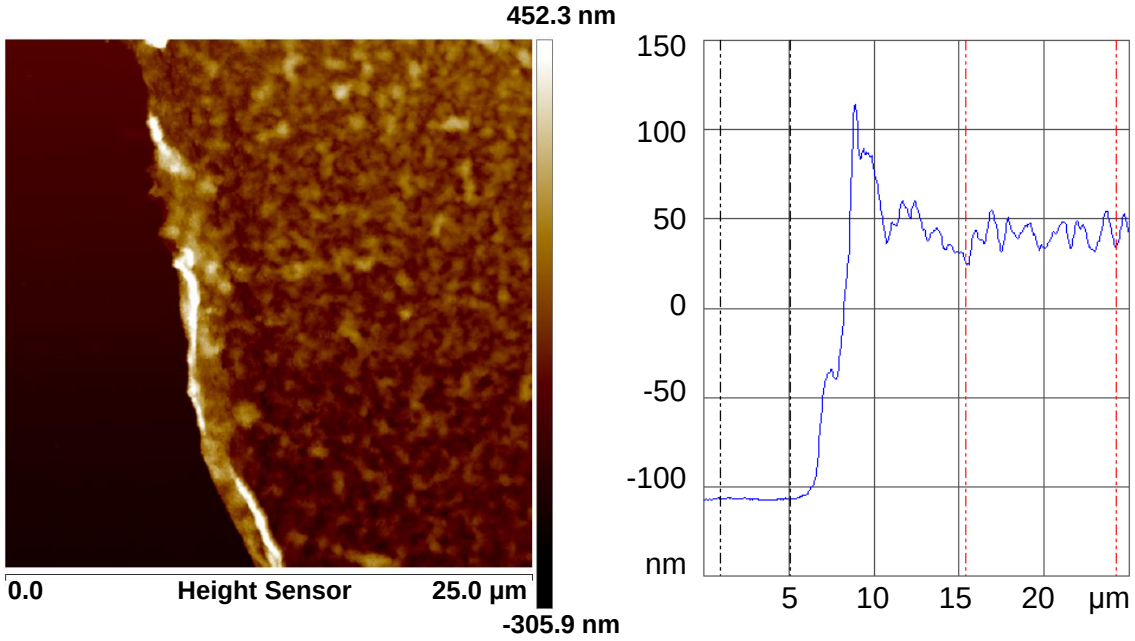

Figure 3. A representative image from AFM characterization of the coated polyamide bilayer studied in this work.

II. Example literature values for the bilayer mass transport model

a) Polyvinyl alcohol

Ref	Description	S	$D \times 10^9$ [m^2/s]
1	M_W* = 79200, 99.6% hydrolyzed (DuPont Elvanol), 23ºC, Physically crosslinked …	~8	0.52
2	Simulated, 400 monomers in each PVA chain, 19.85ºC		
	Non-crosslinked ……..		2.97×10^{-2}
3	High M_W, (type 72-60), < 1.5 % acetate groups. (DuPont Elvanol), 39.8 ºC,		
	Non-crosslinked …...……...	10.5	1×10^{-2}
4	M_W = 105600 to 110000, 99.8 % hydrolyzed. (DuPont Elvanol), Non-crosslinked …….....	≈ 3.95 ± 0.03	0.125 ± 0.015
	Non-crosslinked, thermally treated…..……	≈ 1.64 ± 0.05	0.134 ± 0.027
	Molar crosslink ratio (with glutaraldehyde)		
	X = 0.03…….....	6.02 ± 0.04	0.058 ± 0.002
	X = 0.05…….....	4.48 ± 0.03	0.101 ± 0.010
	X = 0.07…….....	3.35 ± 0.21	0.157 ± 0.010
	X = 0.10…….....	2.25 ± 0.09	0.082 ± 0.011
5	M_W = 31 to 50K, 98 to 99 % hydrolyzed. (Aldrich. Cat. No 36313-8),		

	Non-crosslinked …….....	1.13	2.4
	Chemically crosslinked ……...	1.05	1.0
6	(Preparation not described)		
	< 2 % residual acetyl		
	RH = 40 %	39	5.1×10^{-2}
	RH = 60 %	48	1.25
7	M_W = 160000 (mass average), (Air Product & Chemicals), chemically crosslinked with hydrophilic urethane		
	RH = 38 %	~ 1.039	9.4×10^{-4}
	RH = 61 %	~ 1.079	1.4×10^{-3}
	RH = 74 %	~ 1.119	2.4×10^{-3}

* M_W - mass average molecular weight

b) Polyamide – Diffusion coefficient

Ref	**Description**	***D* [m^2/s]**
8	Crosslinked, aromatic poly(*m*-phenylene trimesamide), RH = 100 %	$\approx 3.76 \times 10^{-12}$
9	Crosslinked, aromatic poly(*m*-phenylene trimesamide), RH = 100 %	$\approx 2.2 \times 10^{-12}$ - 3.3×10^{-12}

III. Validation of the bilayer mass uptake model

To validate the bilayer mass uptake model, we tested two cases of the bilayer mass transport model that should resemble a single layer and compared them with the mass transport behavior solution is given by Equation (A.4) as the water vapor activity is reduced from 0.50 to 0.35. In the first case, the two layers have the same material properties (D = 1×10^{-6} m^2/s, K = 0.1) and therefore act as one layer whose thickness is the sum of the two layers ($L_1 + L_2$ = 2×10^{-7} m, $L_1 = L_2$). In the second case, the material properties are the same and layer 1 has the same thickness, but now layer 2 has thickness L_2 = 2×10^{-22} m. In this case, transport in the second layer becomes vanishingly small and the mass transport in layer 1 should follow Equation (A.4).

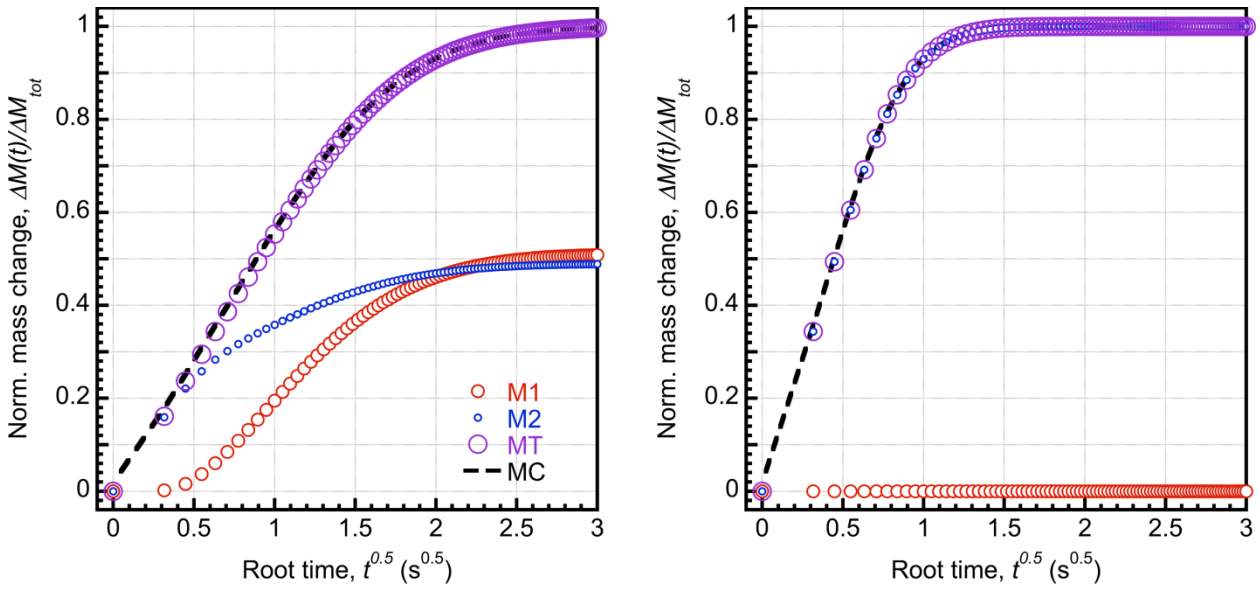

Figure 4. *Left*: Comparison of sorption kinetics for the two layers with the same thicknesses and material properties with Crank's solution for a slab with the same material properties and total thickness. *Right*: Comparison of the solution to the bilayer mass transport model where layer 1

has near zero-thickness with Crank's solution for a slab with the same material properties as layer 2.

IV. Fits of the bilayer mass uptake model to QCM-D data

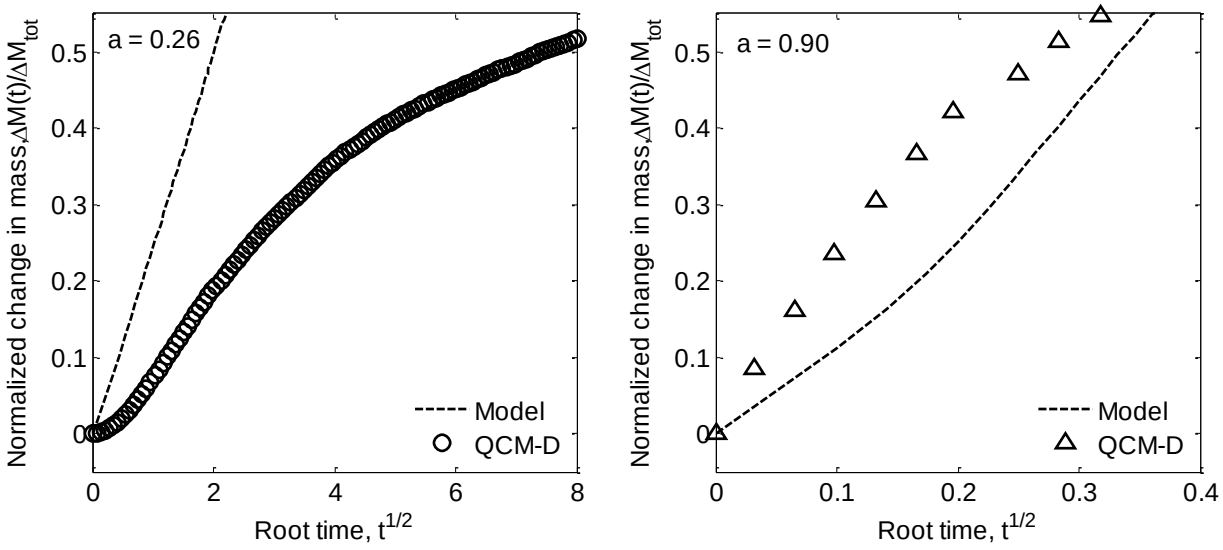

Figure 5. Fit of bilayer mass transport model to QCM-D data using the values in Fig. 5(a) in the manuscript for water activity, a_w = 0.26 (left) and a_w = 0.90 (right). The sum of square errors (SSE) between the fit and QCM-D data for a normalized change in mass up to 0.5 was calculated for ten evenly spaced data points at a_w = 0.26, 0.51, 0.76, and 0.90. The associated SSE are 1.608, 1.524, 1.084, and 0.136. The bilayer mass transport model more accurately fits the experimental data for higher a_w as the period over which normalized change in mass predominantly comes from the PA layer is larger (thus allowing for a more accurate fit).

V. Mathematica code for bilayer mass transport model solution implementation

Notes:

1. This code requires `RootSearch.m`, a Mathematica package that looks for roots ('`EIG`' in the code below) of an equation between '`xmin`' and '`xmax`'.

2. The following quantities must be provided:

Variable	Description
`L1`	Thickness of the layer on the impermeable substrate
`L2`	Thickness of the *bilayer*
`D1`	Diffusion coefficient of the layer between 0 and L_1
`D2`	Diffusion coefficient of the layer between L_1 and L_2
`K1`	Solubility of the layer between 0 and L_1
`K2`	Solubility of the layer between L_1 and L_2

3. The Mathematica code has been provided by the text on numbered lines (not including the numbers). Comments are provided on non-enumerated lines in **(* comment *)** format.

(* Material properties listed in Instructional Note 2 must be provided *before* lines 1-3. *)

```
1  D = (D2/D1)^1/2;
2  L = L1/L2;
3  K = K2/K1;
```

(* Roots to the determinant function (Eq A15) are neither monotonic nor equally spaced between singularities. Therefore, a successful search for eigenvalues (`EIG`) may require a different values for `xmax`, `InitialPrecision`, and `InitialSamples`. *)

```
xmin = 0;
xmax = 1000000;
RSF = RootSearch[D K Cot[(1-L)(EIG^(1/2))]-Tan[D L (EIG^(1/2))]-]==0, {EIG, xmin,
   xmax}, InitialPrecision→ 1, InitialSamples→ 2000];

λ = RSF[[All, 1, 2]];                    (* List of eigenvalues found in (xmin, xmax) *)

f1[v_]:= Sin[(1-L) v^(1/2)]Cos[D z v^(1/2)];    (* Equation A14 *)
f2[v_]:= Sin[(1-z) v^(1/2)]Cos[D L v^(1/2)];    (* Equation A14 *)

g1[v_, w_]:= Exp[-v w];                  (* Equation A9 (without coefficients) *)
g2[v_, w_]:= Exp[-v w];                  (* Equation A9 (without coefficients) *)

C10=K1 C20; (* Initial concentration in Layer 1 at t = 0: CO1 = K2 )
C20=K2 CS0; (* Initial concentration in layer 2 at t = 0: CSO = 1.0* )

f10=1-C10/(K1 CS);                       (* Equation A2 *)
f20=1-C20/(K2 CS);                       (* Equation A2 *)

A[v_]:=(Integrate[f10 f1[v], {z, 0, L}] + K Integrate[f20 f2[v], {z, L,
   1}])/(Integrate[f1[v] f1[v], {z, 0, L}] + K Integrate[f2[v] f2[v], {z, L,
   1}]);                                 (*Equation A16 *)
```

```
17 nmax = 30;                                    (* nmax must be less than the length of λ (Ln 6) *)

18 y1[τ_]:= Sum[A[λ[[n]]] f1[λ[[n]]] g1[λ[[n]], τ], {n,1,nmax}]; (* Equation A17 *)

19 y2[τ_]:= Sum[A[λ[[n]]] f2[λ[[n]]] g2[λ[[n]], τ], {n,1,nmax}]; (* Equation A17 *)
```

(* Lines 20-23: Re-dimensionalization of the concentration functions. *)

```
20 c1=K1 CS(1-y1[τ]);

21 c2=K2 CS(1-y2[τ]);

22 c1D=c1/.{z→x/L2, τ→(D2/(L2^(1/2)))t};

23 c2D=c2/.{z→x/L2, τ→(D2/(L2^(1/2)))t};
```

```
24 M1 = Integrate[c1D, {x,  0, L1}];      (* Eq 12a *)

25 M2 = Integrate[c2D, {x, L1, L2}];      (* Eq 12b *)

26 MT = M1 + M2;                          (* Total mass uptake. *)
```

References

(1) Stauffer, S. R.; Peppast, N. A. Poly (vinyl alcohol) Hydrogels Prepared by Freezing-Thawing Cyclic Processing. *Polymer* **1992**, 33, 3932-3936.

(2) Müller-Plathe, F. Diffusion of Water in Swollen Poly (Vinyl Alcohol) Membranes Studied by Molecular Dynamics Simulation. *J. Membr. Sci.* **1998**, 141, 147–154.

(3) Long, F. A.; Thompson, L. J. Diffusion of Water Vapor in Polymers. *J. Polym. Sci.* **1955**, 15, 413–426.

(4) Hasimi, A.; Stavropoulou, A.; Papadokostaki, K. G.; Sanopoulou, M. Transport of Water in Polyvinyl Alcohol Films: Effect of Thermal Treatment and Chemical Crosslinking. *Eur. Polym. J.* **2008**, 44, 4098–4107.

(5) Hodge, R. M.; Edward, G. H.; Simon, G. P. Water Absorption and States of Water in Semicrystalline Poly (Vinyl Alcohol) Films. *Polymer* **1996**, 37, 1371–1376.

(6) Hauser, P. M.; McLaren, A. D. Permeation Through and Sorption of Water Vapor by High Polymers. *Ind. Eng. Chem.* **1948**, 40, 112–117.

(7) Shafee, E. E.; Naguib, H. F. Water Sorption in Cross-Linked Poly (Vinyl Alcohol) Networks. *Polymer* **2003**, 44, 1647–1653.

(8) Chan, E. P. Deswelling of Ultrathin Molecular Layer-by-Layer Polyamide Water Desalination Membranes. *Soft Matter* **2014**, 10, 2949–2954.

(9) Jin, Y.; Wang, W.; Su, Z. Spectroscopic Study on Water Diffusion in Aromatic Polyamide Thin Film. *J. Membr. Sci.* **2011**, 379, 121–130.